Surface effects and spin glass state in Co_3O_4 coated $MnFe_2O_4$ nanoparticles

F Zeb[1], M Ishaque[1], K Nadeem[1] , M Kamran[1], H Krenn[2] and D V Szabo[3,4]

[1] Nanoscience and Technology Laboratory, International Islamic University, Islamabad 44000, Pakistan
[2] Institute of Physics, Karl Franzens University, Universitätsplatz 5, A 8010 Graz, Austria
[3] Institute for Applied Materials, Karlsruhe Institute of Technology (KIT), D 76344 Eggenstein Leopoldshafen, Germany
[4] Karlsruhe Nano Micro Facility (KNMF), Karlsruhe Institute of Technology (KIT), D 76344 Eggenstein Leopoldshafen, Germany

E mail: kashif.nadeem@iiu.edu.pk

Keywords: magnetic nanoparticles, spin glass, manganese ferrite, Co_3O_4

Abstract

Surface effects and spin glass state have been studied in Co_3O_4 coated manganese ferrite ($MnFe_2O_4$) nanoparticles by using AC and DC magnetic measurements. Average crystallite size of Co_3O_4 coated $MnFe_2O_4$ nanoparticles was 7 nm as calculated by Debye–Scherrer's formula. Simulated ZFC/FC revealed higher value of effective anisotropy (K_{eff}) $= 5 \times 10^6$ erg cm ^{3} of these nanoparticles as compared to bulk $MnFe_2O_4$ due to enhanced surface effects. Temperature dependent saturation magnetization followed the Bloch's law. Temperature dependent coercivity showed sharp increase below 25 K due to strong surface anisotropy and exchange coupling at interface between ferrimagnetic core and antiferromagnetic surface. For frequency dependent AC-susceptibility, dynamic scaling law fit confirmed the spin glass behavior in Co_3O_4 coated $MnFe_2O_4$ nanoparticles. DC field dependent AC-susceptibility showed the suppression of energy barrier, reduced activation energy and decreased strength of interparticle interactions with increasing DC field. Slow spin relaxation in ZFC protocol further confirmed the presence of spin-glass behavior. All this analysis confirmed the existence of spin-glass behavior as attributed to disordered surface spins and interparticle interactions in these nanoparticles, which gets suppressed after the application of moderate DC field.

1. Introduction

The unique and striking features of magnetic nanoparticles have drawn considerable scientific and technological attention because of their wide range of applications in microwave industry, magnetic recording, refrigeration systems, electrical devices, ferro-fluids, MRI imaging and drug delivery [1–6]. All these practical applications needs to study and understand the physical properties of magnetic nanoparticles, which are mainly depend upon the size, shape and interparticle interactions. In single domain nanoparticles, super-exchange interactions and dipolar interactions are usually dominate. These interactions are strongly depend upon temperature. If these interactions are random and strong below a freezing temperature then a spin glass like state can exist in nanoparticles. The spin-glass behavior due to dipolar interactions among nanoparticles is known as super spin-glass, while spin-glass behavior due to disordered surface spins is called surface spin-glass. The dipolar interactions are weaker than the super-exchange interactions. Experimentally, it is not easy to distinguish between super and surface spin-glass behavior.

$MnFe_2O_4$ nanoparticles exhibits an excellent chemical stability with temperature and time. They possess remarkable properties like size dependent saturation magnetization, prominent magneto-crystalline anisotropy and prominent mechanical hardness that makes them unique from the other spinel ferrites [7–14]. Fine $MnFe_2O_4$ nanoparticles consist of two main parts: a core with ordered magnetic structure and a surface with disordered spins due to crystalline symmetry breaking. Both parts can influence the magnetic properties of these nanoparticles. Balaji *et al* [15] reported strong interparticle interactions in $MnFe_2O_4$ nanoparticles at low temperature which are responsible to produce spin glass state analyzed with the help of frequency dependent AC

susceptibility measurements. Gao *et al* [16] reported superparamagnetism and spin glass state in $MnFe_2O_4$ nanoparticles. They also reported increase in H_c and M_s at low temperatures which is due to strong interparticle interactions. Aslibeiki *et al* [17] reported a lower M_s value for $MnFe_2O_4$ nanoparticles than bulk $MnFe_2O_4$ and strong interparticle interactions can lead to the super spin glass like behavior in these nanoparticles.

Bare $MnFe_2O_4$ nanoparticles tend to agglomerate and attain cluster like appearance with increase in size. These cluster become further magnetize when placed in an external magnetic field and result in a form of stronger attraction among these nanoparticles [18]. The magnetic nanoparticles can be coated with a specific material to avoid interparticle interactions. Aslibeiki *et al* [19] studied the polymer coated $MnFe_2O_4$ nanoparticles and reported that the polymer coating enhanced the saturation magnetization, shifted blocking temperature towards the low temperature and changed strong super spin glass behavior to weak superparamagnetic state. Mdlalose *et al* [20] reported that chitosan coating reduced the M_s value of $MnFe_2O_4$ nanoparticles and enhanced H_c. Therefore coating material can significantly alters the magnetic properties of nanoparticles which mainly depends upon the nature of the coating material. Insitu non-magnetic silica coating can reduce the magnetization of the nanoparticles due to decreased nanoparticle's size and is attributed to existence of canted spins [21, 22]. However, coating on the already prepared nanoparticles can significantly control/reduce the interparticle interactions. On the other side, magnetic coating usually generates core–shell interface interactions that can alter the overall effective anisotropy and magnetic properties of the nanoparticles and improve their thermal stability [23–26].

In this present article, we have used antiferromagnetic Co_3O_4 coating on $MnFe_2O_4$ nanoparticles due to its higher density, melting point and thermal stability that can produce exchange coupling between ferrimagnetic (FiM)/antiferromagnetic (AFM) interfaces to tune magnetic properties of $MnFe_2O_4$ nanoparticles. Srikala *et al* [27] studied the effects of CoO coating on Co nanoparticles and reported that the magnetic properties are strongly depend upon the exchange coupling between the ordered core and disordered shell and on the external applied field. In this article, our prime focus is to investigate the surface effects of Co_3O_4 coating on the magnetic properties of $MnFe_2O_4$ nanoparticles.

2. Experimental

$MnFe_2O_4$ coated nanoparticles with Co_3O_4 have been synthesized by microwave plasma fabrication technique by using a frequency of 2.45 GHz microwave equipment. Co_3O_4 coated $MnFe_2O_4$ nanoparticles were protected by a polymer i.e. PMMA because it is stable at the temperatures after the reaction zone and polymerize immediately under the influence of temperature and the UV radiation stemming from the plasma [28]. The comprehensive fabrication is described in detail elsewhere [29, 30]. Structural phase was identified by x-ray diffraction (XRD) (Bruker D8 Advance instrument) by using Cu-Kα ($\lambda = 0.154$ nm) radiation at ambient conditions. Transmission electron microscopy (TEM) was used for imaging of the nanoparticles. The magnetic measurements were taken by super conducting quantum interface device (SQUID) magnetometer (Quantum Design, MPMS-XL-7) using maximum amplitude of the applied field of ± 5 T within the temperature range of 4.2–300 K. The frequency and DC field dependent AC-susceptibility was also taken with the same magnetometer in the frequency range of 1–1000 Hz in the temperature range from 4.2 to 300 K.

3. Results and discussion

X-ray diffraction (XRD) is widely used for the identification of crystal structure, identification of phase crystallinity and information of lattice parameters of materials. Figure 1(a) represents the XRD spectrum of Co_3O_4 coated $MnFe_2O_4$ nanoparticles placed on aluminum substrate. The observed peaks at $2\theta = 18°$, 30.1°, 35.5°, 43.2°, 53.6°, 57°, 62° and 74° from the (111), (220), (311), (400), (422), (511), (440) and (533) planes, respectively represents the standard XRD pattern of $MnFe_2O_4$ phase (JCPDS Card No. 74-2403). The peaks observed at $2\theta = 19°$, 31° and 36.7° are from (111), (220) and (311) planes, respectively representing Co_3O_4 phase (JCPDS card No. 74-1656). Few peaks of Co_3O_4 are overlapping with the peaks of $MnFe_2O_4$ phase. The percentages of $MnFe_2O_4$ and Co_3O_4 are calculated from relative intensities of XRD peaks which are 75% and 25% for $MnFe_2O_4$ and Co_3O_4, respectively. The average crystallite size of the nanoparticles was calculated by using Debye–Scherrer's formula and found 7 nm.

Transmission electron microscopy (TEM) is a vital technique for confirmation of size and shape of the nanoparticles. Figures 1(b) and (c) shows the TEM images of Co_3O_4 coated $MnFe_2O_4$ nanoparticles at the scales of 20 and 50 nm, respectively. TEM images show that the nanoparticles are spherical in shape but with less agglomeration due to their magnetic nature. The Co_3O_4 coating is clearly visible in TEM image as demonstrated by arrows in the figure 1(b).

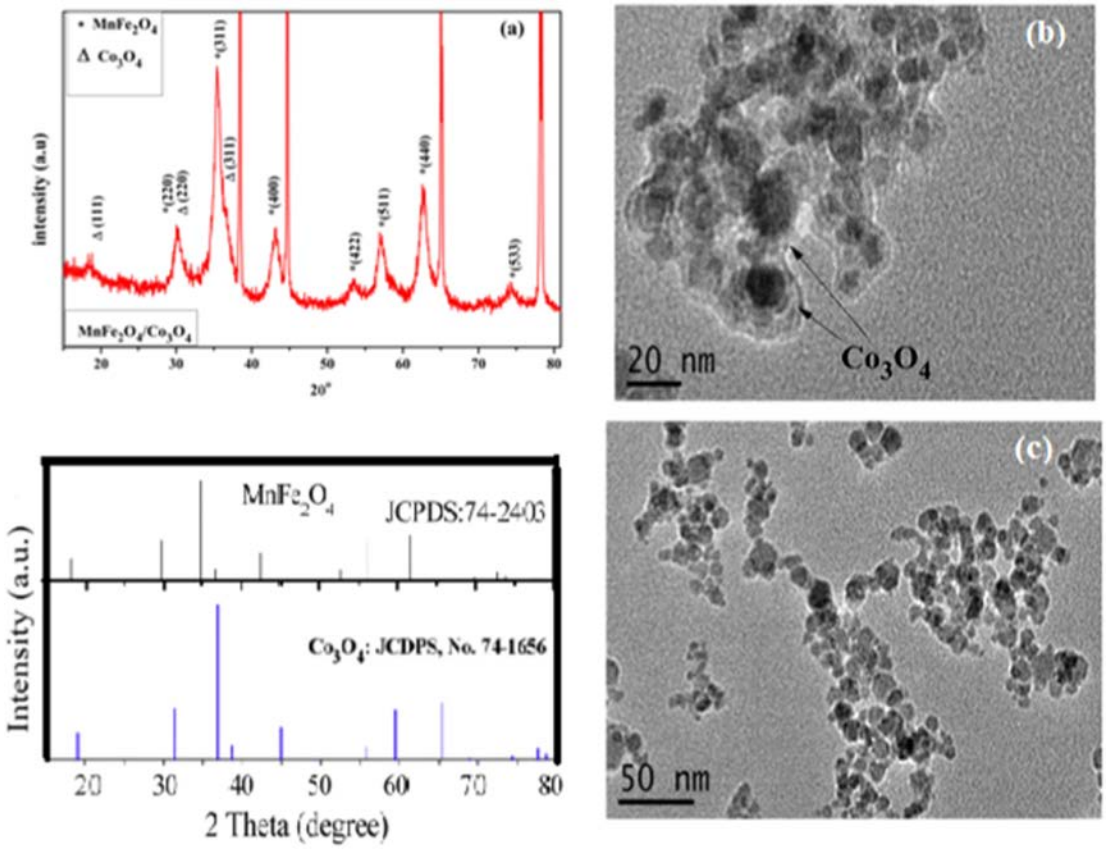

Figure 1. (a) XRD pattern of Co_3O_4 coated $MnFe_2O_4$ nanoparticles with JCPDS cards, (b) TEM image of Co_3O_4 coated $MnFe_2O_4$ nanoparticles at 20 nm and (c) 50 nm scale.

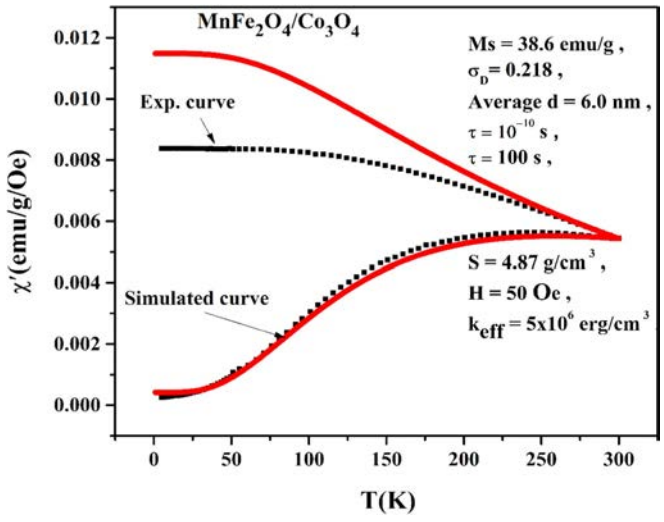

Figure 2. Black squares represents the experimental and red line shows the simulated curves of ZFC/FC of Co_3O_4 coated $MnFe_2O_4$ nanoparticles with obtained simulated parameters.

Figure 2 represents the experimental and simulated zero field cooled (ZFC)-field cooled (FC) curves of Co_3O_4 coated $MnFe_2O_4$ nanoparticles carried out at 50 Oe applied magnetic field. The broad maxima in the ZFC_{exp} curve is observed at ~238 K which represents the average blocking temperature (T_B) of the nanoparticles. In the literature, uncoated $MnFe_2O_4$ nanoparticles of the same size give $T_B \sim 108$ K [31]. This shift of T_B to higher temperature is due to Co_3O_4 coating which increased the magneto-crystalline anisotropy and also the effect of dipolar interactions [32].

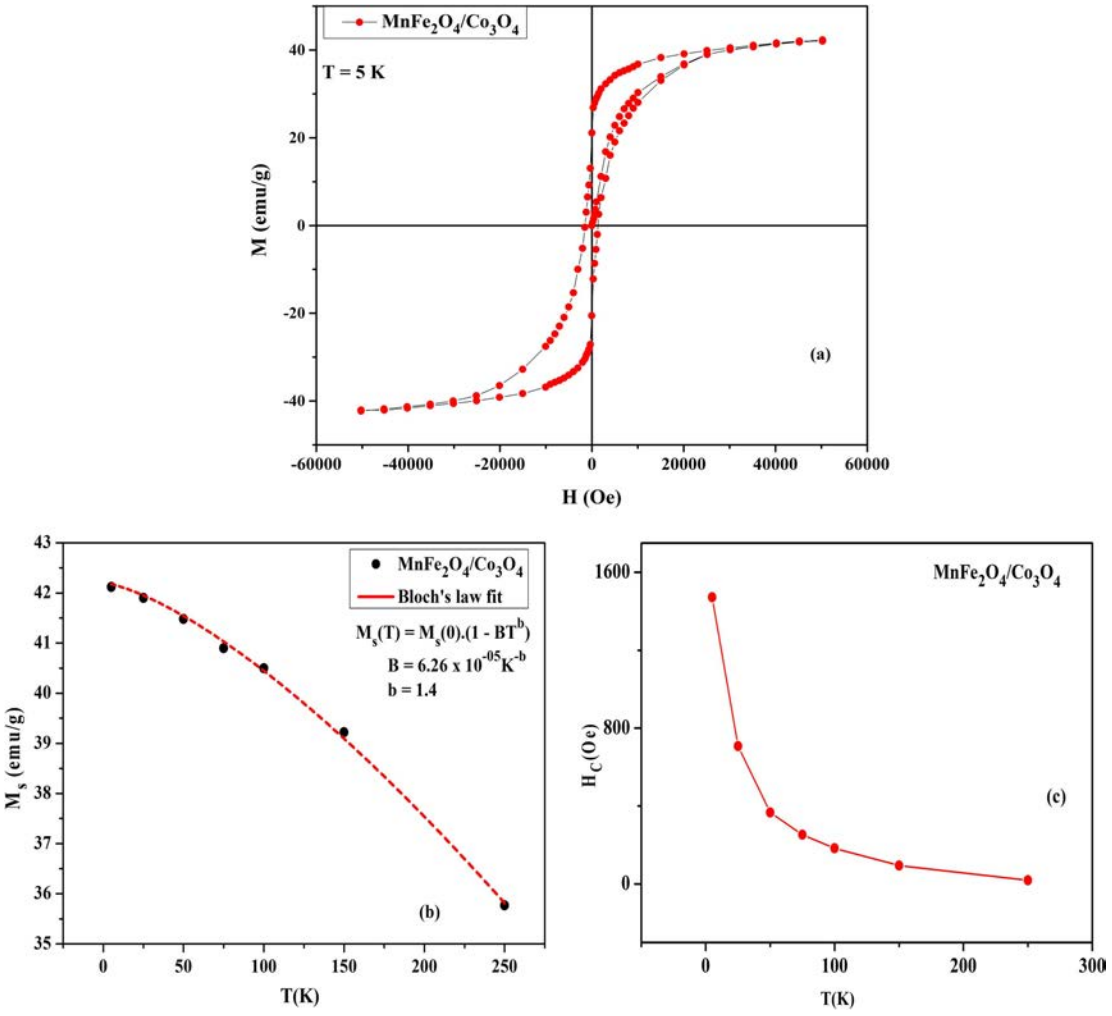

Figure 3. (a) M H loop of Co_3O_4 coated $MnFe_2O_4$ nanoparticles at 5 K (b) temperature dependent saturation magnetization with Bloch's law fit and (c) temperature dependent coercivity.

We have also simulated ZFC and FC susceptibility curves by using Neel-Brown relaxation model. According to this model, ZFC susceptibility can be written as [33],

$$\chi_{ZFC}(T) = \frac{{M_S}^2}{3K_{eff}}\left[\ln\left(\frac{\tau_m}{\tau_0}\right)\int_0^T \frac{T_B}{T} f(T_B)\,dT_B + \int_T^\infty f(T_B)\,dT_B\right] \quad (1)$$

For a certain temperature T, the first and the second term of equation (1) correspond to un-blocked super paramagnetic and stiffed blocked particles, respectively. For FC susceptibility, the same Neel-Brown relaxation model is given as [33],

$$\chi_{FC}(T) = \frac{{M_S}^2}{3K_{eff}}\ln\left(\frac{\tau_m}{\tau_0}\right)\left[\frac{1}{T}\int_0^T T_B f(T_B)\,dT_B + \int_T^\infty f(T_B)\,dT_B\right] \quad (2)$$

The best fit of simulated curve with the experimental curve gives the average particle size $\langle d \rangle = 6$ nm and effective anisotropy constant $K_{eff} = 5 \times 10^{06}$ erg cm ^{3}. The value of K_{eff} for Co_3O_4 coated $MnFe_2O_4$ nanoparticles is higher than the bulk value of $MnFe_2O_4$ ($K_{eff} = 2.5 \times 10^{04}$ erg cm ^{3}) [34] and is attributed to the surface/strain and core-surface interactions effects that dominate the magnetic anisotropy density in these small nanoparticles. The fitted value of K_{eff} of Co_3O_4 coated $MnFe_2O_4$ nanoparticles is also slightly higher than the reported bare $MnFe_2O_4$ nanoparticles (with nearly the same size) which is 2.36×10^6 erg cm ^{3} [31]. The Co_3O_4 coating has leading role in enhancing the K_{eff} value due to coupling between FiM core and AFM surface [32]. The difference arises between the simulated and experimental FC curves is due to the limitation of our model because it is valid for the non-interacting single domain magnetic nanoparticles. Below 30 K, FC_{exp} curve becomes flat. Flattening of the FC_{exp} curve is the sign of spin-glass behavior and/or inter-particle interactions in these magnetic nanoparticles [35, 36].

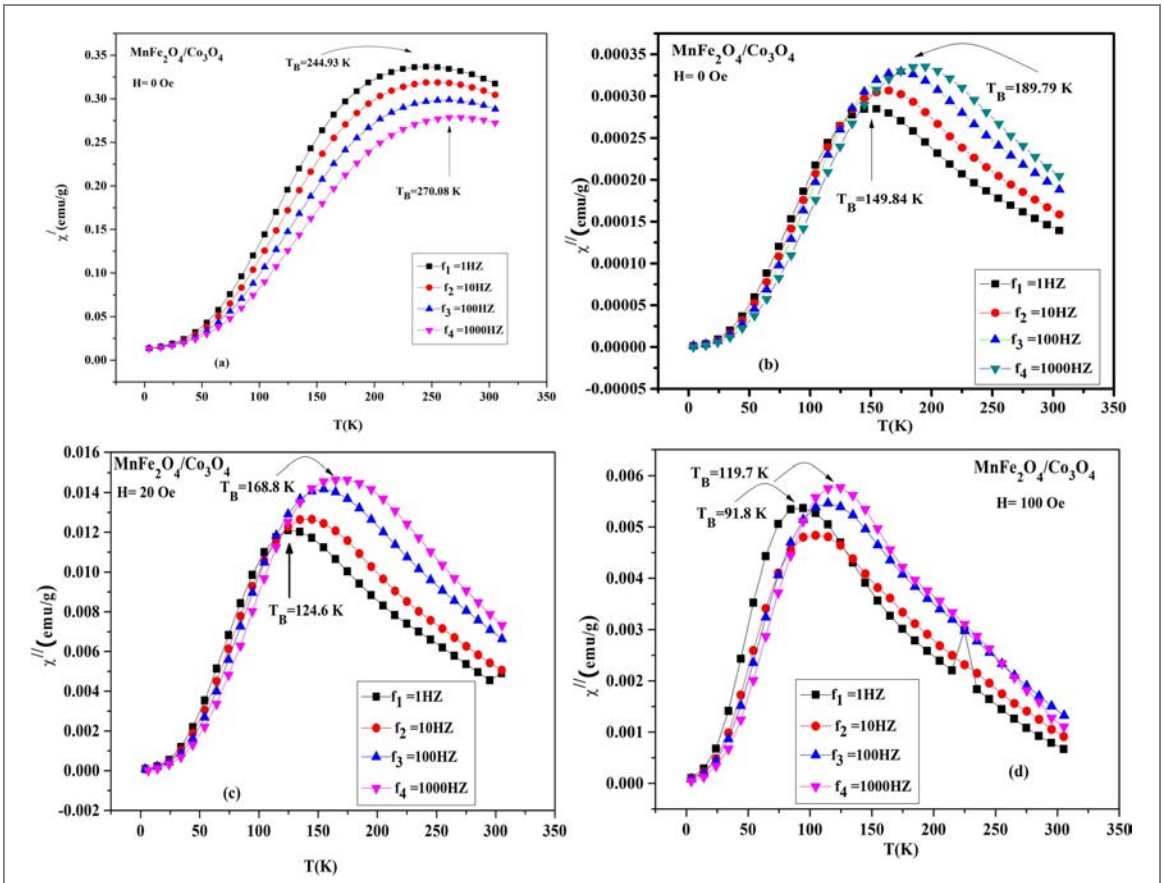

Figure 4. (a) In phase and (b) (d) out of phase parts of frequency dependent AC susceptibility of Co_3O_4 coated $MnFe_2O_4$ nanoparticles under different applied DC fields (H_{DC}) 0 Oe, 20 Oe and 100 Oe, respectively.

Figures 3(a)–(c) shows the M-H loop at 5 K under the applied field of ±5 T, temperature dependent saturation magnetization (M_s) and coercivity (H_c) of Co_3O_4 coated $MnFe_2O_4$ nanoparticles. Maximum M_s value (43 emu g^{-1}) is observed at 5 K, which is less than that of the bulk value [37]. In ferrite nanoparticles, it is common to have reduced M_s value with decreasing particle size because of the disordered or canted surface spins and due to presence of AFM wt% of Co_3O_4 phase in the normalization of magnetization in units of emu/g.

Figure 3(b) shows the temperature dependent M_s for Co_3O_4 coated $MnFe_2O_4$ nanoparticles. It shows an increasing trend with decreasing temperature which is due to reduction in thermal fluctuations. The obtained data is fitted by using Bloch's law and is given as [38].

$$M_S(T) = M_S(0)(1 - BT^b) \tag{3}$$

Surprisingly, the fitted values obtained from equation (3) for Bloch's exponent and Bloch's constant are 1.4 and 6.26×10^{-05} K^{-b} respectively, which is almost consistent with bulk $MnFe_2O_4$ nanoparticles [39, 40]. The slight difference in Bloch's exponent is due to smaller size of nanoparticles. However for nanoparticles, it was reported that the temperature dependent magnetization follow T^2 law rather than the usual Bloch's $T^{3/2}$ law [41]. The deviation from $T^{3/2}$ law is due to the finite-size effects, lack of surface coordination at the surface of magnetic nanoparticles and the energy gap happening in the density of states [21, 42]. Figure 3(c) represents the temperature dependent coercivity (H_c) which gives large value at low temperatures indicates the clear blocking behavior for the single domain nanoparticles. The nanoparticles give the maximum value of $H_c = 1466$ Oe at 5 K which is approximately four time higher than reported bare $MnFe_2O_4$ nanoparticles ($H_c > 420$ Oe at 5 K) [16] and is attributed to exchange coupling at interface between FiM core and AFM shell [43–45]. In the present case, the data deviates from Kneller's law at low temperatures (not shown here) due to strong magneto-crystalline anisotropy including strain anisotropy, surface anisotropy, shape anisotropy, and exchange coupling between FiM core and AFM shell [46–48].

AC-susceptibility measurements were used to study the dynamic magnetization of the nanoparticles because external excitation frequency and energy barrier both are directly influenced by the relaxation time of AC-susceptibility measurements. Figures 4(a) and (b)–(d) shows the in-phase and out-of-phase parts of AC-susceptibility, respectively in the temperature range from 5 K to 300 K at different frequencies (f) = 1, 10, 100 and 1000 Hz under different applied DC magnetic fields. The average blocking temperature increases with the

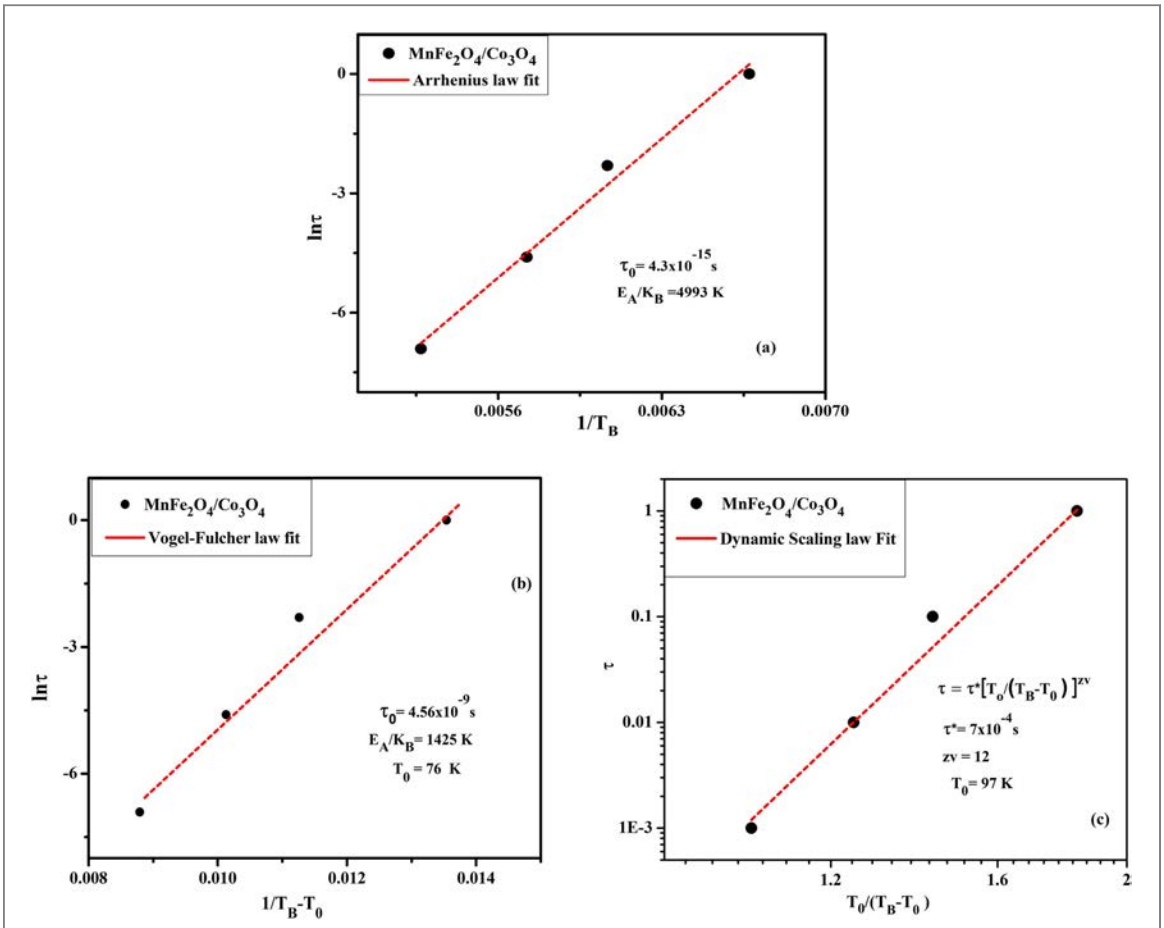

Figure 5. (a) Arrhenius law fit, (b) Vogel Fulcher law fit, and (c) dynamic scaling law fit for Co_3O_4 coated $MnFe_2O_4$ nanoparticles.

increase in frequency due to change of energy barrier (E_A) with applied frequency. For in-phase part at $H_{DC} = 0$ Oe, the T_B shifts from 244 to 270 K as the frequency is increased from 1 to1000 Hz. We have fitted the f-dependence shift of T_B by using different physical laws on out-of-phase part of AC-susceptibility data.

Figures 5(a)–(c) shows the Arrhenius law, Vogel-Fulcher law and dynamic scaling law fits for f-shift of T_B without applied H_{DC}. For thermal excitation of non-interacting single-barrier blocked nanoparticles, Neel-Arrhenius law can be written as,

$$\tau_m = \tau_0 \exp\left(\frac{E_a}{k_B T_B}\right) \tag{4}$$

Where 'E_a' represents the activation energy barrier, 'k_B' be the Boltzmann constant, T_B represents blocking peak temperature and 'τ_o' represents atomic spin-flip time [49]. The values of extracted parameters are $\tau_o = 4.3 \times 10^{-15}$ s and $E_a/k_B = 4993$ K obtained from Arrhenius law fit are unphysical for these nanoparticles. These fitted parameters indicate that Co_3O_4 coated $MnFe_2O_4$ nanoparticles do not follow thermally activated Arrhenius law and therefore they are not non-interacting.

To investigate the interactions between Co_3O_4 coated $MnFe_2O_4$ nanoparticles, Vogel–Fulcher law [50] is commonly used with the additional parameter T_o which represents the strength of interparticle interactions, as given in equation (5)

$$\tau_m = \tau_0 \exp\left(\frac{E_a}{k_B(T_B - T_0)}\right) \tag{5}$$

Figure 5(b) shows the Vogel Fulcher law fit with $T_o = 76$ K. The obtained values for spin flip time and activation energy are $\tau_o = 4.56 \times 10^{-9}$ s and $E_a/k_B = 1425$ K, respectively which are now reasonable for these nanoparticles. The presence of T_o shows that there are moderate interparticle interactions present among these nanoparticles.

For the existence of spin glass behaviour in these nanoparticles, dynamic scaling law is used which can be expressed as,

Table 1. Parameters obtained from physical laws.

Applied field (H) Oe	Laws	Parameters	Values
0	*Arrhenius law*	τ_o	4.3×10^{-15} s
		$\frac{E_A}{k_B}$	4993 K
	Vogel Ful cher law	τ_o	4.5×10^{-9} s
		$\frac{E_A}{k_B}$	1425 K
		T_o	76 K
	Dynamic scal ing law	τ^*	7×10^{-4}s
		zv	12
		T_o	97 K
20	*Arrhenius law*	τ_o	4.2×10^{-14} s
		$\frac{E_A}{k_B}$	3970 K
	Vogel Ful cher law	τ_o	2×10^{-12} s
		$\frac{E_A}{k_B}$	2940 K
		T_o	20 K
	Dynamic scal ing law	τ^*	3.7×10^{-4} s
		zv	7.2
		T_o	96 K
50	*Arrhenius law*	τ_o	5.2×10^{-14} s
		$\frac{E_A}{k_B}$	3508 K
	Vogel Ful cher law	τ_o	3.2×10^{-12} s
		$\frac{E_A}{k_B}$	2563 K
		T_o	18 K
	Dynamic scal ing law	τ^*	1.4×10^{-4} s
		zv	6.17
		T_o	92 K
100	*Arrhenius law*	τ_o	6.5×10^{-13} s
		$\frac{E_A}{k_B}$	2662 K
	Vogel Ful cher law	τ_o	1.9×10^{-11} s
		$\frac{E_A}{k_B}$	1972 K
		T_o	15 K
	Dynamic scal ing law	τ^*	5.2×10^{-4} s
		zv	4.3
		T_o	80 K

$$\tau = \tau^* \left[\frac{T_0}{(T_B - T_0)} \right]^{zv} \tag{6}$$

Where τ^* represents the huge core spin flip time for nanoparticle's spin, which is different from atomic spin flip time. For different magnetic nanoparticles the value of spin flip time lies in the range of 10^{-06}–10^{-09} s [51], T_o is the static transition (freezing) temperature, T_B represents the frequency dependent freezing temperature and 'zv' is the critical exponent which provide the information about the spin-glass state and its ranges from 4 to 12 for different spin-glass systems [52]. The value of spin flip time of these nanoparticles as obtained from dynamic scaling law is $\tau^* = 7 \times 10^{-4}$ s. The higher value of spin flip time τ^* is because of the quenched atomic relaxation of frozen surface spins, dipolar interactions and FiM core-AFM surface interactions. The high value of critical exponent ($zv = 12$) shows that Co_3O_4 coated $MnFe_2O_4$ nanoparticles have magnetic interactions and established spin-glass behaviour.

DC field dependent out-of-phase part of AC-susceptibility of Co_3O_4 coated $MnFe_2O_4$ nanoparticles is shown in figures 4(c) and (d) which shows a peak shift with applying DC field because the energy barrier can be modified (reduced) and nanoparticles spins require less thermal energy to deblock from their anisotropy axes

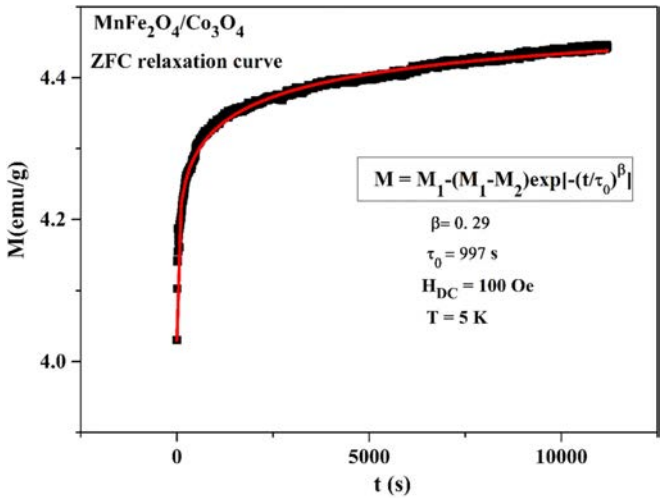

Figure 6. ZFC relaxation curve of Co_3O_4 coated $MnFe_2O_4$ nanoparticles. Red line shows fitting of stretched exponential law curve.

and hence T_B decreases with increasing DC field. We have fitted data of DC field dependent AC-susceptibility with the help of same physical laws (Neel-Arrhenius law, Vogel-Fulcher law and dynamic scaling law) as already used and summarized their obtained parameters in table 1. The values obtained for atomic spin flip time τ_o from Arrhenius law for all the samples increased from 4.3×10^{-15} s to 6.5×10^{-13} s with varying applied DC field from 0 to 100 Oe. It indicates that Co_3O_4 coated $MnFe_2O_4$ nanoparticles exhibit stronger interactions in the absence of applied DC field. With increasing DC field, the interactions between nanoparticles are reduced and shifted towards non-interacting behavior. Applied DC field also reduces interparticle interactions which is confirmed by the decreasing value of effective temperature T_0 with increasing DC field. The activation energy (E_A/k_B) shows decreasing trend from 4993 K to 1972 K with increasing applied DC field. The zv value changes from 12 to 4 with increasing DC field, which shows that DC field have also impact on spin glass state. All these values show that the applied DC field in AC-susceptibility overcomes the interparticle interactions that reduced the blocking temperature and also affect the spin glass state [53–55].

In ferrite nanoparticles, the glassy behavior has been attributed to a super spin glass phase and/or freezing of disordered surface spins. For nanoparticles, time-dependent magnetization is usually expressed in terms of thermally-activated relaxation between two stable magnetization states which are separated by a well-defined energy barrier. Interparticle interactions and spin glass state can modify the energy barrier and they are no longer independent. Superparamagnetic system shows slow spin relaxation in FC protocol only while spin glass system shows slow relaxation in both ZFC and FC protocols. Therefore ZFC relaxation experiment can be beneficial to prove spin glass state. These two states strongly depend upon the value of shape parameter β whose value is lies from 0–1 for different disordered systems [56, 57]. The reported value of shape parameter (β) for spin-glass system lies in the range from 0.2 to 0.6, below the freezing temperature [58]. Figure 6 shows the ZFC relaxation of Co_3O_4 coated $MnFe_2O_4$ nanoparticles at 5 K. Usually relaxation data is fitted by using two well-known models namely stretched exponential decay model and logarithmic relaxation decay model [59]. We have used stretched exponential decay model for ZFC relaxation fitting. For ZFC relaxation, the relation is given as

$$M = M_1 - (M_1 - M_2)\exp[-(t/\tau)^{\beta}] \tag{7}$$

The parameters obtained from the fit are $\beta = 0.29$ and $\tau_o = 997$ s. The shape factor parameter (β) and relaxation time (τ_o) confirmed the slow spin relaxation in these nanoparticles. In Co_3O_4 coated $MnFe_2O_4$ nanoparticles, the spin-glass behavior and stronger interactions causes the slow relaxation. For the system of spin-glass, there are configurational energy barriers and magnetic spins are trapped in system which requires more time for spin-flip.

4. Conclusions

The Co_3O_4 coated $MnFe_2O_4$ nanoparticles were synthesized by using microwave plasma technique. The spinel structure of $MnFe_2O_4$ nanoparticles were confirmed by XRD analysis. TEM images revealed that the Co_3O_4 coated $MnFe_2O_4$ nanoparticles are nearly spherical in shape with less agglomeration. ZFC/FC curves revealed that the K_{eff} value of nanoparticles is higher than the bare and bulk values which is due to enhanced surface anisotropy of these nanoparticles. Surprisingly, The obtained values of fitted parameters from Bloch's law are

$B = 6.26 \times 10^{-05}\ K^{-b}$ and $b = 1.4$ which are in good accordance with that reported for bulk $MnFe_2O_4$ which proved our nanoparticles follow Bloch's law. Coercivity showed a steep increase below 25 K due to blocked surface spins, strong surface anisotropy and exchange coupling at interface between FiM core and AFM surface coating. Vogel-Fulcher law fit gave us a reasonable value of spin flip time and activation energy with $T_o = 76$ K. The value of $\tau^* = 7 \times 10^{-4}$ s and critical exponent $zv = 12$ as obtained from dynamic scaling law fit showed that our nanoparticles exhibited a spin-glass behaviour. DC field dependent AC-susceptibility revealed that blocking temperature, activation energy and atomic spin flip time shifts to lower values due to suppression of energy barrier with applied DC field. The ZFC relaxation of Co_3O_4 coated $MnFe_2O_4$ nanoparticles showed slower magnetic relaxation due to presence of stronger spin-glass behavior in them. All these measurements showed that Co_3O_4 coated $MnFe_2O_4$ nanoparticles revealed enhanced surface spins disorders and magnetic coating does not minimize the surface energy.

Acknowledgments

K Nadeem acknowledges Higher Education Commission (HEC) of Pakistan for financial support. Authors also acknowledge International Islamic University for providing research funds under project no. IIUI/ORIC/RP/HRSC/2016-518.

ORCID iDs

K Nadeem https://orcid.org/0000-0003-3462-2652

References

[1] Gao J, Zhang W, Huang P, Zhang B, Zhang X and Xu B 2008 Intracellular spatial control of fluorescent magnetic nanoparticles *J. Am. Chem. Soc.* **130** 3710 1
[2] Cao H, He J, Deng L and Gao X 2009 Fabrication of cyclodextrin functionalized superparamagnetic Fe_3O_4/amino silane core shell nanoparticles via layer by layer method *Appl. Surf. Sci.* **255** 7974 80
[3] Lee J G, Park J Y, Oh Y J and Kim C S 1998 Magnetic properties of $CoFe_2O_4$ thin films prepared by a sol gel method *J. Appl. Phys.* **84** 2801 4
[4] Pradhan P, Giri J, Samanta G, Sarma H D, Mishra K P, Bellare J, Banerjee R and Bahadur D 2007 Comparative evaluation of heating ability and biocompatibility of different ferrite based magnetic fluids for hyperthermia application *J. Biomed. Mater. Res. Part B: Applied Biomaterials* **81** 12 22
[5] Versluijs J, Bari M and Coey J 2001 Magnetoresistance of half metallic oxide nanocontacts *Phys. Rev. Lett.* **87** 026601
[6] Weller D and Moser A 1999 Thermal effect limits in ultrahigh density magnetic recording *IEEE Trans. Magn.* **35** 4423 39
[7] Deraz N and Alarifi A 2012 Controlled synthesis, physicochemical and magnetic properties of nano crystalline Mn ferrite system *Int. J. Electrochem. Sci.* **7** 5534 43
[8] Lu J, Ma S, Sun J, Xia C, Liu C, Wang Z, Zhao X, Gao F, Gong Q and Song B 2009 Manganese ferrite nanoparticle micellar nanocomposites as MRI contrast agent for liver imaging *Biomaterials* **30** 2919 28
[9] Boni A, Marinone M, Innocenti C, Sangregorio C, Corti M, Lascialfari A, Mariani M, Orsini F, Poletti G and Casula M 2008 Magnetic and relaxometric properties of Mn ferrites *J. Phys. D: Appl. Phys.* **41** 134021
[10] Frey N A, Peng S, Cheng K and Sun S 2009 Magnetic nanoparticles: synthesis, functionalization, and applications in bioimaging and magnetic energy storage *Chem. Soc. Rev.* **38** 2532 42
[11] Lu A H, Salabas E E L and Schüth F 2007 Magnetic nanoparticles: synthesis, protection, functionalization, and application *Angew. Chem. Int. Ed.* **46** 1222 44
[12] Tirosh E, Shemer G and Markovich G 2006 Optimizing cobalt ferrite nanocrystal synthesis using a magneto optical probe *Chem. Mater.* **18** 465 70
[13] Han D H, Luo H L and Yang Z 1996 Remanent and anisotropic switching field distribution of platelike Ba ferrite and acicular particulate recording media *J. Magn. Magn. Mater.* **161** 376 8
[14] Kim D H, Nikles D E and Brazel C S 2010 Synthesis and characterization of multifunctional chitosan $MnFe_2O_4$ nanoparticles for magnetic hyperthermia and drug delivery *Materials* **3** 4051 65
[15] Balaji G, Wilde G, Weissmüller J, Gajbhiye N and Sankaranarayanan V 2004 Spin glass like transition in interacting $MnFe_2O_4$ nanoparticles *Phys. Status Solidi* B **24** 1589 92
[16] Gao R R, Zhang Y, Yu W, Xiong R and Shi J 2012 Superparamagnetism and spin glass like state for the $MnFe_2O_4$ nano particles synthesized by the thermal decomposition method *J. Magn. Magn. Mater.* **324** 2534 8
[17] Aslibeiki B, Kameli P, Salamati H, Eshraghi M and Tahmasebi T 2010 Superspin glass state in $MnFe_2O_4$ nanoparticles *J. Magn. Magn. Mater.* **322** 2929 34
[18] Wang G, Zhao D, Ma Y, Zhang Z, Che H, Mu J, Zhang X and Zhang Z 2018 Synthesis and characterization of polymer coated manganese ferrite nanoparticles as controlled drug delivery *Appl. Surf. Sci.* **428** 258 63
[19] Aslibeiki B, Kameli P, Ehsani M, Salamati H, Muscas G, Agostinelli E, Foglietti V, Casciardi S and Peddis D 2016 Solvothermal synthesis of $MnFe_2O_4$ nanoparticles: the role of polymer coating on morphology and magnetic properties *J. Magn. Magn. Mater.* **399** 236 44
[20] Mdlalose W, Mokhosi S, Dlamini S, Moyo T and Singh M 2018 Effect of chitosan coating on the structural and magnetic properties of $MnFe_2O_4$ and $Mn_{0.5}Co_{0.5}Fe_2O_4$ nanoparticles *AIP Adv.* **8** 056726
[21] Kodama R 1999 Magnetic nanoparticles *J. Magn. Magn. Mater.* **200** 359 72
[22] Respaud M, Broto J, Rakoto H, Fert A, Thomas L, Barbara B, Verelst M, Snoeck E, Lecante P and Mosset A 1998 Surface effects on the magnetic properties of ultrafine cobalt particles *Phys. Rev.* B **57** 2925

[23] Berry C C 2009 Progress in functionalization of magnetic nanoparticles for applications in biomedicine *J. Phys. D: Appl. Phys.* **42** 224003
[24] Zeng H, Sun S, Li J, Wang Z and Liu J 2004 Tailoring magnetic properties of core/shell nanoparticles *Appl. Phys. Lett.* **85** 792 4
[25] Cole A J, Yang V C and David A E 2011 Cancer theranostics: the rise of targeted magnetic nanoparticles *Trends Biotechnol.* **29** 323 32
[26] Iglesias O, Labarta A and Batlle X 2008 Exchange bias phenomenology and models of core/shell nanoparticles *J. Nanosci. Nanotechnol.* **8** 2761 80
[27] Srikala D, Singh V, Mehta B and Patnaik S 2012 Signatures of spin glass freezing in Co/CoO nanospheres and nanodiscs *J. Magn. Magn. Mater.* **324** 2512 8
[28] Vollath D and Szabó D 1994 Nanocoated particles: a special type of ceramic powder *Nanostruct. Mater.* **4** 927 38
[29] Vollath D and Szabó D V 2006 The Microwave plasma process a versatile process to synthesise nanoparticulate materials *J. Nanopart. Res.* **8** 417 28
[30] Szabó D V and Schlabach S 2014 Microwave plasma synthesis of materials from physics and chemistry to nanoparticles: a materials scientist's viewpoint *Inorg.* **2** 468 507
[31] Aslibeiki B, Kameli P and Salamati H 2016 The effect of dipole dipole interactions on coercivity, anisotropy constant, and blocking temperature of $MnFe_2O_4$ nanoparticles *J. Appl. Phys.* **119** 063901
[32] Skumryev V, Stoyanov S, Zhang Y, Hadjipanayis G, Givord D and Nogués J 2003 Beating the superparamagnetic limit with exchange bias *Nature* **423** 850
[33] Denardin J, Brandl A, Knobel M, Panissod P, Pakhomov A, Liu H and Zhang X 2002 Thermoremanence and zero field cooled/field cooled magnetization study of $Co_x(SiO_2)_{1\ x}$ granular films *Phys. Rev.* B **65** 064422
[34] Carta D, Casula M F, Falqui A, Loche D, Mountjoy G, Sangregorio C and Corrias A 2009 A structural and magnetic investigation of the inversion degree in ferrite nanocrystals MFe_2O_4 (M Mn, Co, Ni) *J. Phys. Chem.* C **113** 8606 15
[35] Martinez B, Obradors X, Balcells L, Rouanet A and Monty C 1998 Low temperature surface spin glass transition in γ Fe_2O_3 nanoparticles *Phys. Rev. Lett.* **80** 181
[36] Nakamae S, Crauste Thibierge C, Komatsu K, L'Hôte D, Tahri Y, Vincent E, Dubois E, Dupuis V and Perzynski R 2010 Superspin glass aging behavior in textured and nontextured frozen ferrofluid *J. Appl. Phys.* **107** 09E135
[37] Balaji G, Gajbhiye N, Wilde G and Weissmüller J 2002 Magnetic properties of $MnFe_2O_4$ nanoparticles *J. Magn. Magn. Mater.* **242** 617 20
[38] Chaudhari N, Kambale R, Bhosale D, Suryavanshi S and Sawant S 2010 Thermal hysteresis and domain states in Ni Zn ferrites synthesized by oxalate precursor method *J. Magn. Magn. Mater.* **322** 1999 2005
[39] Chen J, Sorensen C, Klabunde K, Hadjipanayis G, Devlin E and Kostikas A 1996 Size dependent magnetic properties of $MnFe_2O_4$ fine particles synthesized by coprecipitation *Phys. Rev.* B **54** 9288 (1996)
[40] Aquino R, Depeyrot J, Sousa M, Tourinho F, Dubois E and Perzynski R 2005 Magnetization temperature dependence and freezing of surface spins in magnetic fluids based on ferrite nanoparticles *Phys. Rev.* B **72** 184435
[41] Morrish A 1965 *The Physical Principles of Magnetism* (New York: Wiley) Series on the Science and Technology of Materials
[42] Mandal K, Mitra S and Kumar P A 2006 Deviation from Bloch $T^{3/2}$ law in ferrite nanoparticles *Europhys. Lett.* **75** 618
[43] Van der Zaag P, Ijiri Y, Borchers J, Feiner L, Wolf R, Gaines J, Erwin R and Verheijen M 2000 Difference between blocking and Néel temperatures in the exchange biased Fe_3O_4/CoO system *Phys. Rev. Lett.* **84** (2000) 6102
[44] Geshev J 2000 Analytical solutions for exchange bias and coercivity in ferromagnetic/antiferromagnetic bilayers *Phys. Rev.* B **62** 5627
[45] Berry S, Lind D, Chern G and Mathias H 1993 Magnetization changes with modulation period in Fe_3O_4/NiO superlattices *J. Magn. Magn. Mater.* **123** 126 32
[46] Dmitriev A and Filatov A 2017 Generality of spontaneous and stimulated magnetization reversal in MnSb clusters embedded in GaMnSb thin films *Phys. Solid State* **59** 1734 8
[47] Issa B, Obaidat I M, Albiss B A and Haik Y 2013 Magnetic nanoparticles: surface effects and properties related to biomedicine applications *Int. J. Mol. Sci.* **14** 21266 305
[48] Wernsdorfer W, Orozco E B, Hasselbach K, Benoit A, Barbara B, Demoncy N, Loiseau A, Pascard H and Mailly D 1997 Experimental evidence of the Néel Brown model of magnetization reversal *Phys. Rev. Lett.* **78** 1791
[49] Néel L 1952 Théorie du traînage magnétique de diffusion *J. Phys. Radium* **13** 249 64
[50] Dormann J L, Fiorani D and Tronc E 2007 Magnetic relaxation in fine particle systems *Adv. Chem. Phys.* **98** 283 494
[51] Kumar D and Banerjee A 2013 Coexistence of interacting ferromagnetic clusters and small antiferromagnetic clusters in $La_{0.5}Ba_{0.5}CoO_3$ *J. Phys.: Condens. Matter* **25** 216005
[52] Reimer L 2013 *Transmission Electron Microscopy: Physics of Image Formation and Microanalysis* (Berlin: Springer)
[53] Fu Z, Zheng Y, Xiao Y, Bedanta S, Senyshyn A, Simeoni G G, Su Y, Rücker U, Kögerler P and Brückel T 2013 Coexistence of magnetic order and spin glass like phase in the pyrochlore antiferromagnet $Na_3Co(CO_3)_2Cl$ *Phys. Rev.* B **87** (2013) 214406
[54] Azad A K, Sanchez Benitez J and Irvine J T 2013 Spin glass transition in $La_{0.75}Sr_{0.25}Mn_{0.5}Cr_{0.5\ x}AlxO_{3\ \delta}$ perovskites *Mater. Res. Bull.* **48** 2482 90
[55] Balanda M 2013 AC susceptibility studies of phase transitions and magnetic relaxation: conventional, molecular and low dimensional magnets *Acta Phys. Pol.* A **124** 964 76
[56] Wang F, Zhang J, Chen Y F, Wang G J, Sun J R, Zhang S Y and Shen B G 2004 Spin glass behavior in La $(Fe_{1\ x}Mn_x)_{11.4}$ $Si_{1.6}$ compounds *Phys. Rev.* B **69** 094424
[57] Zeb F, Nadeem K, Shah S K A, Kamran M, Gul I H and Ali L 2017 Surface spins disorder in uncoated and SiO_2 coated maghemite nanoparticles *J. Magn. Magn. Mater.* **429** (2017) 270 5
[58] Bhattacharyya A, Giri S and Majumdar S 2011 Spin glass like state in GdCu: role of phase separation and magnetic frustration *Phys. Rev.* B **83** 134427
[59] Fisher D S and Huse D A 1986 Ordered phase of short range Ising spin glasses *Phys. Rev. Lett.* **56** 1601